Operational Research in Engineering Sciences: Theory and Applications
Vol. 6, Issue 2, 2023, pp. 238-269
ISSN: 2620-1607
eISSN: 2620-1747
DOI: https://doi.org/10.31181/oresta/060213

RESEARCH ON FORMATION CONTROL AND DYNAMIC FORMATION TRANSFORMATION STRATEGY OF MOBILE ROBOTS IN COMPLEX SCENARIOS

Yanjie Cao*, Norzalilah Mohamad Nor

School of Mechanical Engineering, Universiti Sains Malaysia (USM), 14300 Nibong Tebal, Pulau Pinang, Malaysia.

Received: 19 April 2023
Accepted: 19 May 2023
First Online: 22 July 2023

Research Paper

***Abstract**: In this paper, we propose a mobile robot formation control method and an efficient formation transformation strategy for an engineering problem where mobile robot formation transformation is inflexible in a complex obstacle environment. First, kinematic and positional models of differentially mobile robots are designed for accurate control of robot formation; Second, an improved leader-follower formation method for introducing virtual robots is designed, and the data set for robot formation avoidance strategy is proposed by considering the obstacle data in the environment comprehensively, which lays the foundation for dynamic robot formation transformation; Finally, a formation strategy with a robot formation scaling factor ρ and a robot formation dynamic transformation factor σ is designed. This strategy can quickly determine the position of each robot in the formation through the parameter matrix of the target formation based on the information of obstacles in the environment detected by the robot, thus realizing the dynamic transformation of the robot formation. We have verified its effectiveness through computer simulation and physical experiments. The strategy of this paper realizes the robot formation through the complex obstacle environment, and successfully realizes the functions of formation maintenance, isomorphic deformation, heterogeneous deformation and scattered obstacles crossing obstacles.*

***Keywords**: Mobile robot; Topological structure; Leader–Follower; Multi-mobile robot system; Formation transformation.*

*Corresponding Author: caoyanjie@student.usm.my (Y. Cao)

1. Introduction

A multi-robot system is a regular formation sequence of multiple individuals in a certain way, and they work together to complete tasks through mutual cooperation. The advantages of multi-robot systems are reflected in the following: (1). A multi-robot system accomplishes tasks through a distributed working model, within which the robots can share their own resources with access to information, thus significantly increasing efficiency. (2). Multi-robot systems allow for a more comprehensive inspection of the environment. (3). When faced with complex tasks, multi-robot systems can collaborate with each other to compensate for their lack of capability. (4). When performing complex tasks, multi-robot systems have better flexibility and robustness.

Multi-robot formation technology has been widely used in many fields, especially in complex and changeable obstacles. For example, In logistics, the e-commerce platform, Amazon, has made warehousing intelligent through collaboration between handling robots, greatly improving efficiency, shown as Figure 1.

Figure1. Logistics robot formation operation site

This paper focuses on the problem of formation change when multiple robots encounter obstacles, so that the multi-robot group can quickly and dynamically avoid obstacles according to the environmental constraints and achieve effective avoidance of obstacles during the formation operation.

The innovations of this paper are as follows:

1. The kinematics control model of robot formation is designed, which improves the accuracy of formation control.
2. In this paper, the position and angle of each robot in the formation and the real-time pose of the robot are defined by using the mathematical model. A quantitative data set is formed. This can improve the efficiency of robot formation deformation.
3. The obstacle avoidance strategy of dynamic formation transformation of multi-mobile robots is designed, which can realize the functions of isomorphic deformation, heterogeneous deformation, formation maintenance and scattered obstacle crossing, and effectively deal with complex obstacles.

2. Literature Review

Compared with single mobile robot operation, multi-robot formation has the advantages of high cooperation, strong fault tolerance and high efficiency. Therefore,

multi-mobile robot formation system have been widely used in industrial fields (Gao et al., 2018), such as smart factories, logistics and transportation, unmanned inspection, cooperative handling and other application scenarios. Multi-robot formation control, as the most important problem in the field of swarm robots, forms a multi-robot cooperative mechanism through the mutual positioning of multi-robots to respond to the tasks of the system efficiently. The main purpose of multi-machine cooperation mechanism is to design a control protocol, so that robots can maintain stable formation, formation transformation and obstacle avoidance behavior under the action of this control protocol (Yin et al., 2022).

After years of research by scholars in the field of robot formation control, several typical formation control methods have been developed, including: the virtual structure method (Liu & Zhang, 2018), the behavior-based method (Lee & Chwa, 2018), the graph theory method (Issa & Rashid, 2019), and the leader-following method (Chen et al., 2022).

In the virtual structure method, robot formation is regarded as a rigid body structure. In the virtual rigid body structure, each individual has a unique target position. In the formation process, the individual completes the formation by adjusting its own linear velocity and angular velocity to track the target position Rabelo, Brandão, and Sarcinelli-Filho (2018) Yan et al., (2021). proposed a control strategy to steer the formation of two mobile robots (Rabelo et al., 2018; Yan et al., 2021). The strategy corresponds to treating the entire formation as a single virtual structure, which corresponds to a line formation in 3D space. Dibyendu Roy et al. (2018) proposed a region-based shape controller switching strategy for the traditional obstacle avoidance problem in the virtual structure approach (Roy et al., 2018). The initial virtual structure allows the robot to move as a group within a circular region. This helps to form changes in the intelligent

In the behavior-based approach, the formation control task is decomposed into basic behaviors such as driving to the target area, formation generation, and formation maintenance, and the formation motion control of multiple mobile robots is accomplished through behavior fusion (Arrichiello et al., 2010; Hacene & Mendil, 2021). designed a formation control method for robot swarms with behavior-based control to bring the robots together and maintain a specific formation while avoiding obstacles and walls in a dynamic environment Lee and Chwa (2018). proposed a discrete behavior-based multi-robot population control algorithm (Lee & Chwa, 2018). The algorithm uses the relative position information between the robot and the adjacent robot, between the robot and the obstacle, and designs an algorithm based on the behavior method to realize the formation control. The flexibility of multi-robot control based on behavior method needs to be improved because there is no accurate mathematical analysis of the individual and the whole system.

The graph theory approach applied to group formation control is to model the group robots using graph theory knowledge, where each node in the graph represents the motion state of each robot or the motion state of each obstacle Liu and Jiang (2013). proposed a distributed controller based on graph theory that can achieve the formation control goal without assuming any tree-aware structure (Liu & Jiang, 2013). Liang, Sun, and Wang (2017) used graph theoretic approach to determine two time-varying reliability evaluation metrics and proposed a method to evaluate the time-

varying reliability of a collaborative system of multiple underwater robots (Liang et al., 2017).

In the leader-follower method, the navigator plans the movement path of the whole team and leads the movement of the whole formation, while the follower tracks its running trajectory, generates and maintains the formation according to the distance and angle relative to the navigator, and finally realizes the movement of the formation as a whole Halima, Abdelouahab, & Yaakoub, 2018; Park and Yoo (2021). proposed a robust leader-follower formation tracking design method based on connectivity preservation and collision avoidance performance function (Halima et al., 2018; Park & Yoo, 2021). This method enables multiple uncertain under actuated surface ship formations to move steadily. Similarly, Qinhang Jiang and Yan (2022) established the tracking error relationship between the follower and the guide and utilized the PID algorithm to generate the follower's linear velocity (Jiang & Yan, 2022), which solved the problem of guiding-following motion of two line-circulating AGVs.

In addition, (Li, 2021) designed a multi-robot formation control and tracking algorithm based on improved leader follower in wireless sensor environment. The method helps robot formation to remain stable in a perturbed environment (Yaghmaei & Abedi, 2018). proposed a new state space model based on leader-follower formation for non-holonomic mobile robot systems. Furthermore, considering the influence of interference signals (Yan & Fang, 2019), designed a new distributed tracking controller, so that the followers in the formation can estimate the degree of interference to the leader based on the observer, so as to adjust their pose in real time. The leader-follower method is widely used because of its simple method (Liang et al., 2020) and less computation, but its biggest drawback is its poor stability, that is, once the leader cannot move normally due to system failures or algorithm problems, the entire group will fall into stagnation.

Based on the above analysis, we will introduce virtual robots in this paper to improve the leader-following algorithm in order to improve its stability.

The multi-robot formation transformation mainly includes static formation transformation and dynamic formation transformation, among which the most one is the multi-robot dynamic formation transformation problem. One of the more popular methods of avoiding obstacles in multi-robot formations during missions is the flexible avoidance of obstacles through formation changes. Scholars have carried out a series of studies on the formation transformation control of multi-robots in obstacle environments and have achieved many research results.

(Deng et al., 2022) proposed a multivariate D-leader algorithm based on multi-robot formation transformation. On the basis of the Leader-Follower algorithm, the idea of dynamic guidance is introduced to flexibly carry out multi-robot formation and realize the dynamic formation adjustment of guided robots (Jiamin et al., 2022). proposed a hierarchical multi-robot formation control algorithm. Among them, the tactical layer designed the control laws for formation switching motion and different formation keeping motion, and the dynamic window method was used to design the anti-collision strategy during the formation process (Chen et al., 2020). proposed a multi- robot formation control algorithm based on an improved virtual spring method. It enables the robot formation to switch between reach target mode and obstacle avoidance mode according to the distance to the obstacle. As a result, robots can

realize stable formation in complex environments.

The purpose of robot formation change is that the multi-robot system receives instructions to change from the initial formation to a specified formation in order to meet the mission requirements (Wasik et al., 2016). explored a graph-based framework to achieve control of real robot formations moving in a world cluttered with a variety of obstacles by introducing a new distributed algorithm for reconfiguring the formation shape. (Tran et al., 2020) extended the negative imaginary number consensus control method to switch the formation shape of the robot while using only the relative distance between agents, combined with the relative distance between agents and obstacles, to investigate a new method for invariant formation control when switching for a set of heterogeneous autonomous vehicles. Turpin et al. (2021) proposed the CAPT algorithm, which is a combination of centralized and improved distributed algorithms, in which the robot's trajectory is controlled without collisions, but the optimization of the formation transformation is not considered in the algorithm.

In practice, multi-robot collaborative operations are often constrained by the real environment, and the current multi-robot handling environment is relatively simple, and the main consideration in formation control is the interrelationship between the robots, with less consideration given to the interaction between the formation members and the environment.

In summary, there are some limitations in the research on robot formation transformation. Most of the methods do not sufficiently consider the problem of formation transformation and the efficiency of formation transformation in conjunction with environmental constraints. In a practical environment, robots in formation performing some kind of task will inevitably encounter obstacles. In order to avoid the obstacles, the robots in the formation need to dynamically change the formation in real time according to the environmental constraints. In this paper, we focus on the dynamic formation change based on environmental constraints. By establishing the kinematic and positional models of differential mobile robots and introducing the pilot-follower algorithm of virtual robots to realize the formation control of multi-mobile robots. The mathematical matrix is designed to define the position and angle of each robot in the formation and the real-time pose of the robot. A quantitative data set is formed. The multi-robot formation can flexibly change formation to avoid obstacles according to the constraints of the surrounding environment. And designing the formation strategy with robot formation expansion factor ρ and robot formation dynamic transformation factor σ, we finally realize the efficient transformation of multi-mobile robot formation in complex obstacle environment. The other sections of this paper are the arrangement: Section 3 describes how to establish the motion model of differential mobile robot and discloses the establishment of the leader-follower formation algorithm model. Section 4 shows the obstacle avoidance strategy of multi-robot dynamic formation transformation. Section 5 presents the experiments and discussions. Section 6 shows the conclusions and future works.

3. Methodology

3.1 Differential Mobile Robot Motion Model

3.1.1 Kinematics Model Construction

The kinematics model of mobile robot is a mathematical model formed by simplifying and abstracting the running state and motion characteristics of the robot. Through the analysis of the model, the relationship between the position and speed of the robot can be calculated (Saleh et al., 2018).

3.1.1.1 Analysis of Coordinate Transformation of Mobile Robot

The coordinate system of mobile robot includes global coordinate system and robot coordinate system (Li & Chou, 2018). In general, the center position of the robot can be set as the origin. The transformation relationship between the two is shown in Figure 2.

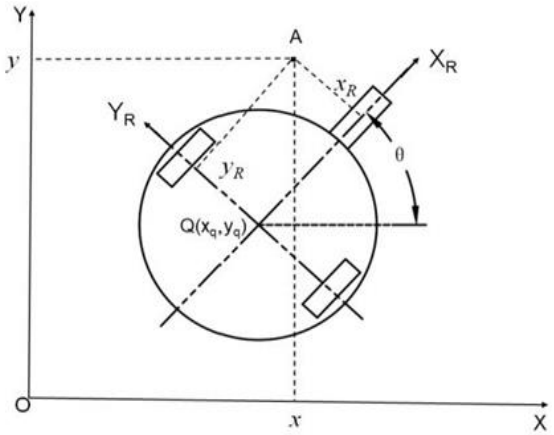

Figure2.Robot coordinate system transformation diagram

The robot center point Q is set as the origin of the robot coordinate system, and A is any position point in the current environment. The transformation relationship of point A in the world coordinate system and the robot coordinate system is shown in Formula (1).

$$\begin{cases} x = x_q + x_R \cos\theta - y_R \sin\theta \\ y = y_q + x_R \sin\theta + y_R \cos\theta \end{cases} \quad (1)$$

Where x, y are the coordinates of point A in the global coordinate system, xR, yR are the coordinates of point A in the robot coordinate system, and θ is the azimuth angle of the robot.

3.1.1.2 Kinematics Model of Mobile Robot

The two-wheel differential mobile robot is the simplest form of mobile robot, so it is one of the most widely used research objects in academic research. According to the motion constraint relationship, the two-wheel differential mobile robot belongs to a non-holonomic constraint motion system model (Fu et al., 2018). Therefore, when the mobile robot reaches a certain position, its running rate will be limited, and the corresponding kinematic model is shown in Figure 3.

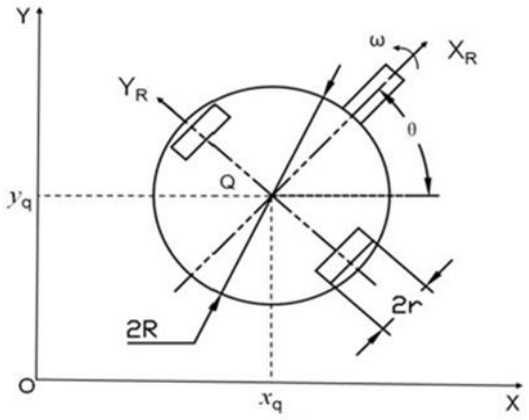

Figure3.Kinematics model of mobile robot

Let $p = [x, y, \theta]^T$, the kinematic equation is shown in Equation (2):

$$\dot{p} = \begin{bmatrix} \dot{x} \\ \dot{y} \\ \dot{\theta} \end{bmatrix} = \begin{bmatrix} \cos\theta & 0 \\ \sin\theta & 0 \\ 0 & 1 \end{bmatrix} \begin{bmatrix} v \\ w \end{bmatrix} \quad (2)$$

where Q is the robot centroid; $\dot{x}$、$\dot{y}$、$\dot{\theta}$ and represent the linear velocities of point Q in the global coordinate system in the X,Y and Z directions, respectively; Use $w = \dot{\theta}$ to represent its angular velocity and define the counterclockwise direction as positive; Use v to represent the linear velocity of point Q in the robot coordinate system.

$$u = [v, w]^T \quad (3)$$

$$H(p) = \begin{bmatrix} \cos\theta & 0 \\ \sin\theta & 0 \\ 0 & 1 \end{bmatrix} \quad (4)$$

Then its equation of state is

$$\dot{p} = H(p)u \quad (5)$$

where $u = [v, w]^T$ and (w_L, w_R) satisfy the relation:

$$\begin{bmatrix} v \\ w \end{bmatrix} = \begin{bmatrix} \frac{1}{2}r & \frac{1}{2}r \\ \frac{r}{2R} & \frac{r}{2R} \end{bmatrix} \begin{bmatrix} w_L \\ w_R \end{bmatrix} \quad (6)$$

Bringing equation (6) into equation (3) yields:

$$\dot{p} = \begin{bmatrix} \dot{x} \\ \dot{y} \\ \dot{z} \end{bmatrix} = \begin{bmatrix} \frac{1}{2}r\cos\theta & \frac{1}{2}r\cos\theta \\ \frac{1}{2}r\sin\theta & \frac{1}{2}r\sin\theta \\ \frac{r}{2R} & -\frac{r}{2R} \end{bmatrix} \begin{bmatrix} w_L \\ w_R \end{bmatrix} \quad (7)$$

3.1.2 Mobile Robot Posture Model Construction

Aiming at the pose perception requirements of mobile robots, a pose calculation model is established, which is the basis of robot formation. The odometer can calculate the real-time pose state of the mobile robot in the global coordinate system.

Its working principle is the encoder mounted on the drive motor is used to determine its rotation angle, so as to calculate the real-time pose change of the robot during motion (Dudzik, 2020).

The pose of the robot in the formation at any time t_i is $X_i = [x_i, y_i, \theta_i]^T$, Then the pose at $t_i + 1$ is $X_{i+1} = [x_{i+1}, y_{i+1}, \theta_{i+1}]^T$ The number of lines of the encoder in the odometer is Z。If the left and right wheels output pulse signals Δt in time are N_L and N_R respectively, ignoring the phenomenon of wheel slip during the movement, the driving distances are (8).

$$\begin{cases} \Delta x_L = \frac{2\pi r N_L}{z} \\ \Delta x_R = \frac{2\pi r N_R}{z} \end{cases} \quad (8)$$

where, Δx_L、Δx_R respectively, for the left and right driving wheel driving distance in time.

The formula (8) can be obtained:

$$\begin{cases} w_L = \frac{2\pi r N_L}{z\Delta t} \\ w_R = \frac{2\pi r N_R}{z\Delta t} \end{cases} \quad (9)$$

Combining equation (8) and equation (9) yields the direction of rotation of the mobile robot as in equation (10):

$$\Delta\theta = \frac{2\pi r(N_L, N_R)}{2ZR} \quad (10)$$

Therefore, it is known that：

1). when $\Delta\theta = 0$, Mobile robot driving in a straight line.

2). when $\Delta\theta > 0$, Mobile robots turn clockwise and drive.

3). when $\Delta\theta < 0$, The mobile robot turns and drives counterclockwise.

Combining the above equations, it can be deduced that the position state of the mobile robot at the moment $t_i + 1$ is X_{i+1}.

$$\begin{bmatrix} x_{i+1} \\ y_{i+1} \\ z_{i+1} \end{bmatrix} = \begin{bmatrix} x_i \\ y_i \\ z_i \end{bmatrix} + \begin{bmatrix} \cos(\theta_i + \Delta\theta) & 0 \\ \sin(\theta_i + \Delta\theta) & 0 \\ 0 & 1 \end{bmatrix} \begin{bmatrix} \frac{\pi r(N_L, N_R)}{z} \\ \Delta\theta \end{bmatrix} \quad (11)$$

3.2 Leader-Follower Formation Algorithm Modeling

3.2.1 Leader-Follower Formation Structure Model

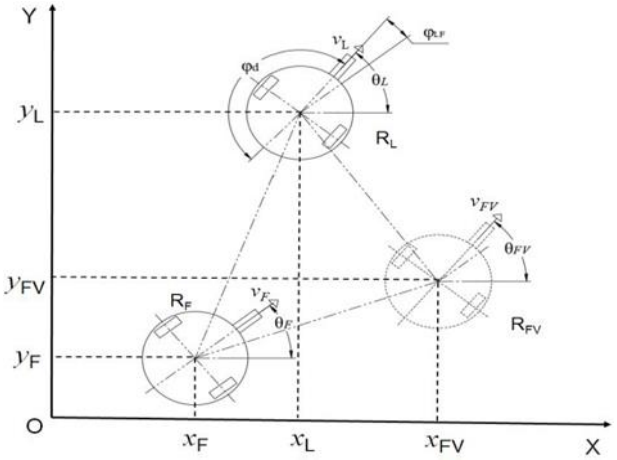

Figure4.Kinematic model of leader-follower formation with the introduction of virtual robots

To represent the position of each robot member in the formation, the geometric structure model of the formation needs to be designed, and the more widely used leader-follower method is used in this paper for formation control (Raghuwaiya et al., 2018). And the virtual robot is introduced in it to keep the formation in line with the pilot robot at all times. The virtual robot determines the ideal position of the following robot; the ideal operating position of the pilot robot is determined by the fused sensor data; and the specific position relationship is derived from the corresponding pilot-following formation mathematical model, which is shown in Figure 4.

Under the global coordinate system XOY, the meanings of the parameters in Figure 4 are as table1.

Table 1. Formation operation model parameters

Parameters	Description
$\mathbf{R_L}$	leader, position (x_L, y_L, θ_L)
$\mathbf{R_F}$	follower, position (x_F, y_F, θ_F)
$\mathbf{R_{FV}}$	Virtual Followers, position $(x_{FV}, y_{FV}, \theta_{FV})$
$\boldsymbol{\theta_L}$	Angle between navigator speed and horizontal axis
$\boldsymbol{\theta_F}$	The angle between the virtual follower speed and the horizontal axis
$\boldsymbol{\theta_{FV}}$	Angle between follower velocity and horizontal axis
$\mathbf{I_d}$	Distance of virtual followers relative to the leader
$\boldsymbol{\varphi_d}$	Directional angle of the virtual follower relative to the navigator
$\mathbf{I_{LF}}$	The distance of followers relative to navigators
$\boldsymbol{\varphi_{LF}}$	The directional angle of the follower relative to the navigator

Then the control goal of the formation is to be able to satisfy the following control law for any of the following robots R_F:

$$\lim_{t\to\infty}(R_{FV} - R_F) = 0 \quad (12)$$

The expected formation matrix of the followers R_F at this point: $E = \begin{bmatrix} R_L & 0 & 0 \\ R_F & l_d & \varphi_d \end{bmatrix}$

By translating and calculating the poses of the navigator R_L, the positional expression of the virtual following robot R_{FV} in the global coordinate system can be derived as (13).

$$\begin{cases} x_{FV} = x_L + l_d \cos(\theta_L + \varphi_d) \\ y_{FV} = y_L + l_d \sin(\theta_L + \varphi_d) \\ \theta_{FV} = \theta_L \end{cases} \quad (13)$$

The actual position of the follower can be represented by the navigator position, as shown in Equation (14).

$$\begin{cases} x_F = x_L + l_{LF} \cos(\theta_L + \varphi_{LF}) \\ y_F = y_L + l_{LF} \sin(\theta_L + \varphi_{LF}) \\ \theta_F = \theta_F \end{cases} \quad (14)$$

Expression for the positional error of the following robot R_F relative to the virtual following robot R_{FV} (15).

$$\begin{cases} \Delta x = x_{FV} - x_F \\ \Delta y = y_{FV} - y_F \\ \Delta\theta = \theta_{FV} - \theta_F \end{cases} \quad (15)$$

Based on the fact that the positional error relationship between the following robot and the virtual following robot is derived from the global coordinate system, it needs to be converted to an error equation in the following robot's own coordinate system, which is conducive to controlling the robot's motion. The expression of the converted positional error (16) can be obtained.

$$e_F = \begin{bmatrix} e_x \\ e_y \\ e_\theta \end{bmatrix} = \begin{bmatrix} \cos\theta_F & \sin\theta_F & 0 \\ -\sin\theta_F & \cos\theta_F & 0 \\ 0 & 0 & 1 \end{bmatrix} \begin{bmatrix} \Delta x \\ \Delta y \\ \Delta\theta \end{bmatrix} = Te^{\Delta} \quad (16)$$

Where：T is the transformation matrix. Substituting (13), (14) and (15) into (16), we can get (16).

$$e_F = \begin{bmatrix} e_x \\ e_y \\ e_\theta \end{bmatrix} = \begin{bmatrix} l_d \cos(e_\theta + \varphi_d) - l_{LF} \cos(e_\theta + \varphi_{LF}) \\ l_d \sin(e_\theta + \varphi_d) - l_{LF} \sin(e_\theta + \varphi_{LF}) \\ \theta_L - \theta_F \end{bmatrix} \quad (17)$$

Where e_x, e_y, e_θ is the tracking trajectory error of follower R_F and virtual follower R_{FV} in the robot coordinate system. And the transformation matrix T is a full rank matrix, that is, RANK $(T) = 3$ for any θ_L. Therefore, the above transformation is equivalent linear transformation, T is invertible.Then there exists T−1 such that $e^{\Delta} = T^{-1}e_F$, $e_F \to 0$equivalent to $e^{\Delta} \to 0$, Therefore, the control trajectory tracking error tends to zero to obtain the desired formation. The kinematic equation of the trajectory tracking difference can be obtained by deriving Formula (17).

$$e_F = \begin{bmatrix} e_x \\ e_y \\ e_\theta \end{bmatrix} = \begin{bmatrix} V_L \cos e_\theta - V_F + e_y w_F - w_L l_d \sin(e_\theta + \varphi_{LF}) \\ V_L \sin e_\theta - e_x w_F + w_L l_d \cos(e_\theta + \varphi_{LF}) \\ w_L - w_F \end{bmatrix} \quad (18)$$

Using the robot formation structure model, any formation structure can be described. Through the introduction of the virtual following robot RFV, the formation keeping problem is transformed into the tracking problem between RF and RFV, and then the formation keeping problem of the robot formation composed of n robots can be transformed into the tracking problem between n-1 robots.

3.2.2 Build quantitative data set of formation.

In order to describe specific leader-follower relationships and formation shape information control. In this paper, a mathematical model is used to define the position and angle of each robot in the formation and to describe the real-time pose of the robot. In this way, a quantitative dataset is formed that enables multi-mobility robot formation to quickly generate target formation shapes required by environmental changes during movement (Akman, 2014).

The leader in the specified formation is responsible for planning and coordinating the motion of the whole system, while the follower can track the leader first when the leader can be detected within the sensor sensing range, which can prevent the cumulative propagation of formation error. When the leader of the formation is out of the detection range of a follower due to the limitation of sensors and communication range, or the leader of the formation is blocked by other robots, the follower chooses its predecessor as the leader, which makes the formation robust to communication failure. In this paper, a directed acyclic graph (Li et al., 2019) is used to represent a scalable formation. Each robot can be regarded as a vertex, and the relationship between two robots is regarded as an edge. Each robot has a unique identity, called nRID (robot ID), and the robot uses its nRID number as its subscript, such as R1, R2, etc. The nRID is used to determine the position of the robot in the formation, where the nRID of the leader of the formation is 1, and the other robots in the formation are follower robots (nRID = 2,3 ·· n). In order to express the relationship between the robots and the shape parameters of the formation, the formula of the parameter information matrix of the formation shape is defined as (19) and (20):

$$F_d = [F_{s1}\ F_{s2}\ ..F_{sn}]_{4\times n} \quad (19)$$

$$F_{sj} = [f_{1j}\ f_{2j}\ \ f_{3j}\ f_{4j}]^T \quad (20)$$

Where: $j = 1 \ldots n; f_{1j} = j;\ f_{2j} = i;\ f_{3j} = l_{ij}^d;\ f_{4j} = \varphi_{ij}^d, F_d$ represents the parameter information matrix of a formation shape, and its member F_{sj} represents the formation information of the jth robot $R_j . F_{sj}$ consists of four parts : f_{1j} is the nRID number of a specific follower robot $R_{j.}$; f_{2j} is the nRID number of the leader tracked by $R_{j.}$ in the current formation ; f_{3j} represents the desired distance between the following robot R_j and its leader, and f_{4j} is the desired direction angle between the following robot R_j and its leader. Since R_1 is designated as the leader of the formation, F_{s1} = $[1\ 0\ 0\ 0]^T$.

By defining the formation parameter matrix set as F = {fi $|F_1^d, F_w^d, F_c^d, F_t^d\}$ to represent the current formation library formation. The common formation parameter

matrix in the quantitative data set can be written as formulas (21), (22), (23), (24).

$$F_1^d = \begin{bmatrix} 1 & 2 & .. & j & .. \\ 0 & 1 & .. & \mathrm{j}-2 & .. \\ 0 & l_j^d & .. & l_j^d & .. \\ 0 & \frac{\pi}{2} & .. & \frac{\pi}{2}+(\mathrm{j}\%2) & .. \end{bmatrix}_{4\times n} \quad (21)$$

$$F_w^d = \begin{bmatrix} 1 & 2 & .. & j & .. \\ 0 & 1 & .. & \mathrm{j}-2 & .. \\ 0 & l_j^d & .. & l_j^d & .. \\ 0 & \frac{3\pi}{2} & .. & \frac{3\pi}{4}+\frac{\pi}{2}+((j+1)\%2) & .. \end{bmatrix}_{4\times n} \quad (22)$$

$$F_c^d = \begin{bmatrix} 1 & 2 & .. & j & .. \\ 0 & 1 & .. & \mathrm{j}-1 & .. \\ 0 & l_j^d & .. & l_j^d & .. \\ 0 & \pi & .. & \pi & .. \end{bmatrix}_{4\times n} \quad (23)$$

$$F_t^d = \begin{bmatrix} 1 & 2 & .. & j & .. \\ 0 & 1 & .. & \mathrm{j}-2 & .. \\ 0 & l_j^d & .. & l_j^d & .. \\ 0 & \frac{3\pi}{4} & .. & \frac{3\pi}{4}+\frac{\pi}{2}+(j\%2) & .. \end{bmatrix}_{4\times n} \quad (24)$$

where "%" is the remainder operation.

3.2.3 Robot formation controller design

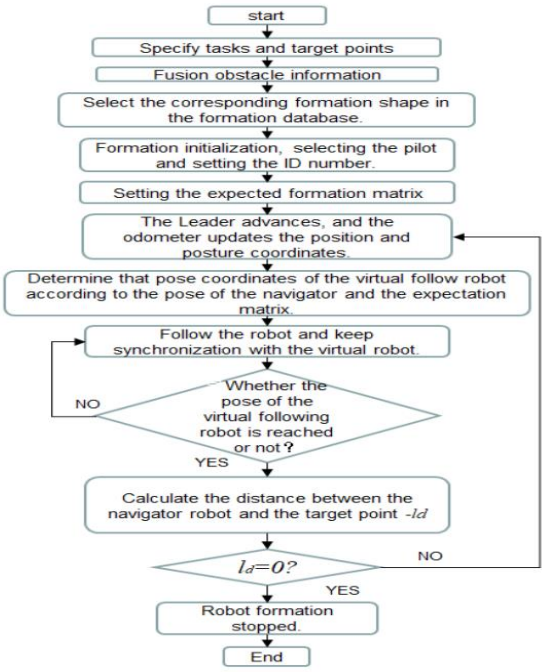

Figure5.Flow chart of robot formation control algorithm

According to the idea of the improved virtual structure leader-follower method, the specific implementation steps of the formation algorithm can be obtained.

Step 1: The program starts, specifying the mission and target point.

step 2: The pilot acquires information about surrounding obstacles, makes a judgment, and selects a suitable formation shape in the database.

Step 3: Select a robot as the pilot robot and set the ID identification number matrix R= [1 2 3...n], where ID number "1" is the pilot robot and ID number "2 $\cdots n$" are the following robots.

Step 4: Build the desired formation matrix E based on the set desired formation.

Step 5: The pilot robot keeps moving towards the target point and updates the position information according to the odometer feedback data.

Step 6: Determining the virtual following robot positional coordinates based on the results of steps 4 and 5.

Step 7: The following robot takes the coordinates of the following virtual following robot's poses as its own target point in the formation, constantly adjusts its own poses to maintain the formation, keeps the following robot and the virtual robot synchronized, and judges whether the error between them is zero.

Step 8: Continuing to execute step 7; if synchronization is not achieved, and step 9 if synchronization is achieved.

Step 9: Calculate the distance I_d between the pilot robot and the target point.

Step 10: If I_d = 0, then the robot formation stops; if $I_d \neq 0$, then continue to execute step 5. The flow chart of the virtual structure leader-follower formation algorithm is shown in Figure 5.

4. Multi-mobile Robot Dynamic Formation Transformation Obstacle Avoidance Strategy

4.1 Calculation of the Width of the Obstacle Course

When the mobile robot formation passes through a complex environment, it is necessary to use the airborne light detection and ranging (LiDAR) to detect the obstacle environment in front of it and calculate the maximum width of the obstacle area. Among them, the leading robot plays a role of decision-making control, judging how the current area should pass, and completing the generation of passable paths. At the same time, it publishes the control coefficient of the following robot, commands the formation to carry out formation transformation, and then realizes multi-aircraft formation obstacle avoidance.

4.1.1 Complex Obstacle Environment Recognition

The robot formation will monitor the distance of obstacles in the surrounding environment in real time to avoid collision caused by untimely formation change. During the formation change process, the maximum safe collision avoidance distance between two robots is set in order to avoid collision caused by the distance between the robots. When the robot detects the existence of obstacles in the environment, the formation program starts to calculate the passable width and starts the corresponding obstacle avoidance strategy according to the width size.

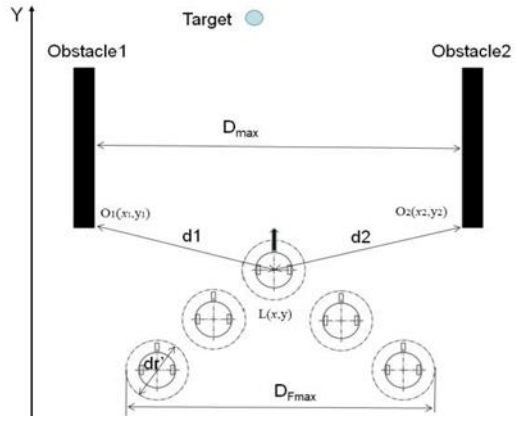

Figure6.Calculation of the passage width of mobile robot formation

4.1.2 Robot Formation Passing Width Calculation

As shown in Figure 6, a robot formation wants to pass an environment with obstacles on both sides and needs to calculate the distance to the obstacles and the passable width. The specific calculation is as (25) to (27).

$$d_1 = \sqrt{(x - x_1)^2 + (y - y_1)^2} \quad (25)$$

$$d_2 = \sqrt{(x - x_2)^2 + (y - y_2)^2} \quad (26)$$

$$D_{max} = \sqrt{(x_1 - x_2)^2 + (y_1 - y_2)^2} \quad (27)$$

where

d_1, d_2 are the distances from the robot to the obstacles 1 and 2, respectively.

D_{max} is the maximum gap distance between the two obstacles, which is the passable distance.

D_{Fmax} is the overall width of the robot formation.

d_r' is the maximum theoretical size of a single mobile robot.

Similarly, when there are enough obstacles in the environment, the calculation is as (28) to (30).

$$d_m = \sqrt{(x - x_m)^2 + (y - y_m)^2} \quad m = 1,3,5 \ldots .2i + 1 \quad (28)$$

$$d_n = \sqrt{(x - x_n)^2 + (y - y_n)^2} \quad n = 2,4,6 \ldots .2i \quad (29)$$

$$D_{max}(m,n) = \sqrt{(x_m - x_n)^2 + (y_m - y_n)^2} \quad (30)$$

where

d_m、d_n are the distances from the robot to the obstacles m and n, respectively.

$D_{\max(m,n)}$ is the maximum gap distance between two obstacles m and n.

When the mobile robot formation wants to pass through the obstacle area on both sides, it needs to judge the environment according to the detection distance, and then calculate the passable width, and if it is passable, the midpoint of the connecting line is chosen as the safe path point that the formation must pass.

4.2 Mobile Robot Formation Dynamic Transformation Strategy

In this section, four different formation transformation strategies are proposed for

obstacle avoidance: formation hold, scattered crossing formation transformation, formation isomorphic transformation, and formation heterogeneous transformation. The design increases the formation stretching transformation factor ρ and formation transformation coefficient σ, so that when the formation encounters different obstacles, it can fully consider the environmental constraints and dynamically select the formation transformation strategy suitable for formation avoidance.

Definition 1: Formation expansion factor is a parameter that allows a formation of multiple robots to maintain its existing shape and expand only in size, denoted by the symbol ρ, $\rho > \rho t$ and the threshold value of the formation expansion factor (the minimum value of the expansion factor that ensures that the robots in the formation do not collide), which is calculated as follows:

$$\rho = \frac{D_{max}}{D_{Fmax}} \quad (31)$$

where, denotes the maximum width of the robot formation, and is the maximum width of the passable path formed by the obstacles in front of the robot formation running route in the obstacle environment, as shown in Figure 6.

The workflow of the dynamically optimized formation transformation obstacle avoidance strategy is shown in Figure 5. During the movement of the whole robot formation toward the target point, the pilot robot relies on the laser sensor it carries to sense the surrounding environment information and obtain the passable area between the current position and the target point to determine the desired path of the whole formation. If this desired path is located between two obstacles ($D_{max} > 0$), the current formation stretch factor ρ can be calculated, and the specific value of the stretch factor σ, is used to determine the formation transformation mode coefficient of obstacle avoidance, according to which the coefficient enters the formation transformation mode.

i. Scattered obstacle crossing

When the robot formation detects that the width of the passage between obstacles is less than the width of the robot formation and the width of the obstacles themselves is less than the width of the individual robots, the robot formation scatter obstacle crossing formation change procedure is initiated. On the basis of maintaining the overall formation of the robot formation, each mobile robot single body will do dynamic fine-tuning to pass through the scattered obstacle zone without consuming too much energy.

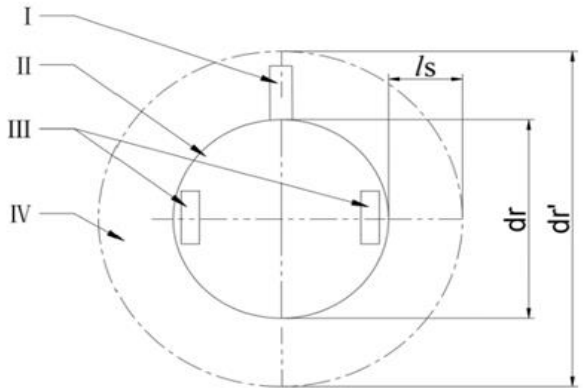

Figure7. Simplified model of differential speed mobile robot

I. Directional sign II. Robotic body III. Differential theory IV. Safe crash zone

Where:

$d_{r'}$ is the maximum theoretical width dimension of the mobile robot mono block.
d_r is the maximum actual width dimension of the mobile robot mono block.
I_s is the safety expansion size of the mobile robot monolithic periphery.

$$d_{r'} = d_r + I_s$$

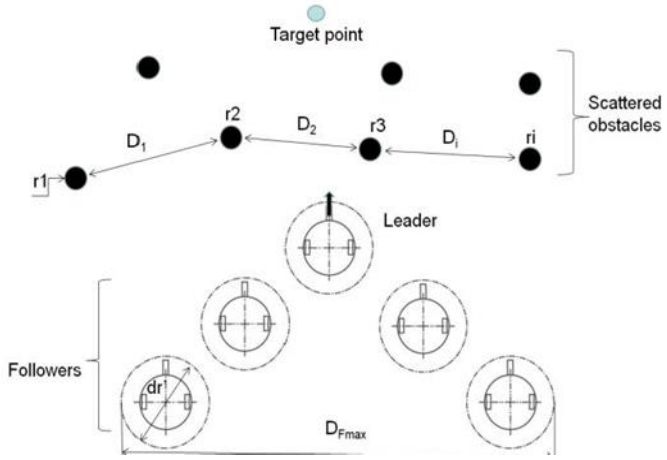

Figure8.Schematic diagram of scattered obstacle crossing decision.

Satisfying equation (32) and equation (33) as follows:
$D_i < D_{Fmax} \leq d_{r'} (i = 1,2 \ldots n)$ (32)
$d_{r'} \geq ri \ (i = 1,2 \ldots n)$ (33)

where :
D_i is the width dimension of the gap between each obstacle r_i is the maximum form factor of each obstacle.
D_{Fmax} is the maximum form factor of the multi-robot formation
D_{Fmin} is the minimum form factor of the multi-robot formation
D_{max} is the dimension of the narrow passage

ii. Narrow passage obstacle crossing.

First, when the narrow aisle width D_{max} , which conforms to the relationship of $d_{r'} < D_{max} < D_{Fmax}$ the robot formation needs to perform distance and angle reduction to make formation changes based on maintaining the basic formation.

Team isomorphic transformation mode (σ = 1):If $\rho < 1$ and $\rho > \rho t$, it means that the robot team cannot pass the obstacle zone directly, but can pass the obstacle zone by compressing the formation size and not changing the formation shape, then set the formation transformation factor σ to 1. The new formation parameter matrix *F1* can be determined by the scaling factor ρ , and this transformation only changes the size of the formation without destroying the original formation structure. At the same time, after the robot team passes through the obstacle zone, the robot members in the formation easily revert to the original formation and continue the task.

Second, the robot formation has the maximum deformation capability to pass through the narrow passage in a straight line formation when the width of the narrow passage D_{max} hich is consistent with the relationship $D_{Fmin} = d_{r'} \leq D_{max}$ eue heterogeneous transformation mode (σ = 2): When the above two modes are not established ($\rho < \rho t$).It shows that only the existing formation of the robot group can pass through the obstacle area. This transformation mode is called formation heterogeneous transformation. At this time, the formation transformation coefficient is set σ to 2. However, what kind of target formation the robot team transforms from the current formation needs to be comprehensively evaluated according to the formation transformation evaluation index proposed in the previous section, so as to obtain the formation parameter matrix F2 of the target formation.

Zero-transformation mode (σ = 0): If $\rho > 1$, $D_{max} > D$ space in front of the pilot robot is large enough, the member robots in the formation can pass the obstacle zone without changing the existing formation shape, which is called zero-transformation, and the formation transformation coefficient σ is set to 0. Zero-transformation does not change the structure of the formation, so it is the optimal solution of the dynamic formation optimization transformation obstacle avoidance strategy.

By obtaining the target formation parameter matrix, the desired position of individual robots can be calculated and then the dynamic formation optimization transformation in the obstacle environment can be implemented. When the last follower in the formation successfully crosses the obstacle zone, the leader robot issues a command to resume the formation, and the individual robots in the formation regroup with their respective leaders as a reference to complete the obstacle avoidance and continue the task.

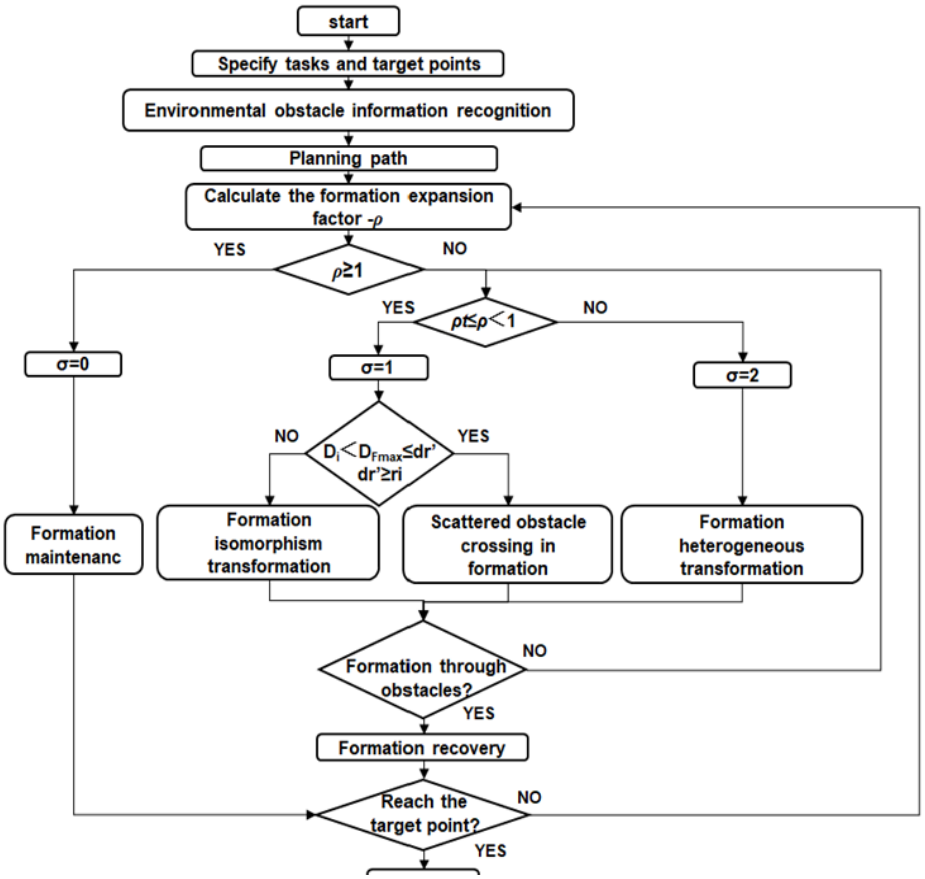

Figure9.Flow chart of mobile robot formation change strategy

5. Experiments Results and Discussion

The goal of this paper is to enable the robot team to dynamically and optimally select the best leader-follower topology through the obstacle zone according to the environmental constraints. The simulation validation is achieved through the MATLAB software platform.

5.1 Simulation Tests

The sampling time interval in the simulation experiment is set to ts=0.1. Considering the performance parameters of the actual robots and the limitations of the robot driver output capability, the control input constraints are as follows:

$0 < v < v_{max}, -\omega_{max} < \omega < \omega_{max}$ (34)

Where: $v_{max} = 0.7$ m/s, $\omega_{max} = 0.1$ rad/s

The trajectory of the navigator robot is determined by equation (35):

$x_r = 20 \cdot t - 50 \cdot \cos(0.1 \cdot t)$ (35)

In addition, initialize x maximum velocity 0.7m/s; y maximum velocity 0.7m/s; x maximum acceleration 0.4m/s^2; y maximum acceleration 0.4m/s^2; The robot formation parameters during the simulation are shown in Table 2.

Table 2. Parameter table of robot formation

Item	Sparameters		
	x	y	θ
Leader	0	0.5	π/4
Follower1	0	1	π/4
Follower2	0	-0.5	-π/4
Follower3	0	-1	π/4
Follower4	0	0	π/4

First, before a multi-robot system can perform formation motion, an initial formation needs to be formed from a random state. Before starting the movement, the robots are located in different areas of the workspace and have no communication with each other. When the formation task is given, each robot in the system needs to move to the target location to form the initial formation. In this paper, we adopt the widely used leader- follower method for formation control and simulate the formation process of mobile robots.

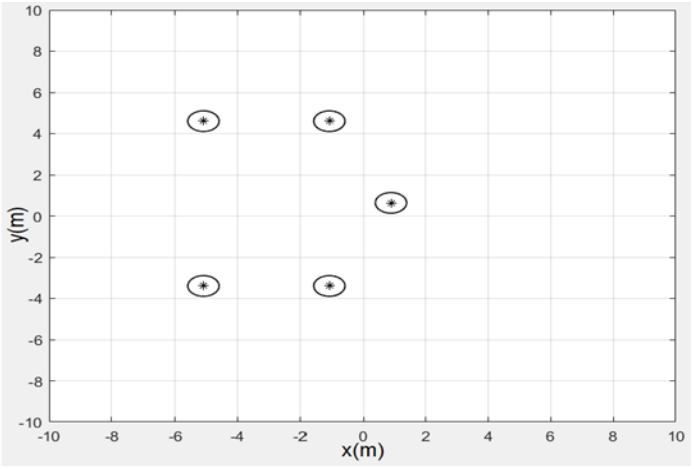

Figure10.Multi-mobile robot formation shaping diagram

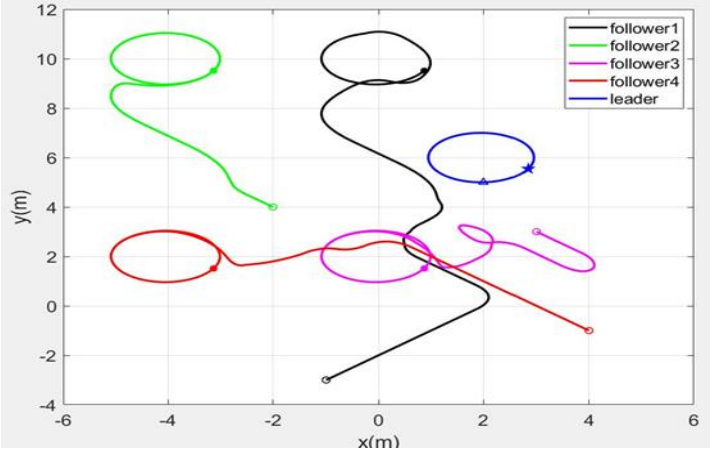

Figure11.Multi-robot formation trajectory diagram.

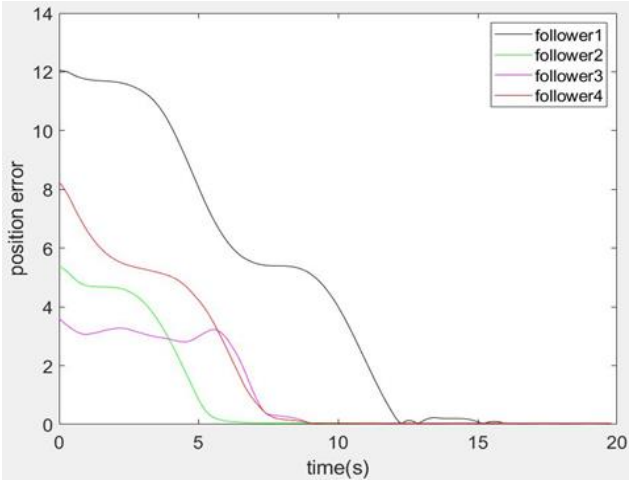

Figure12. Multi-robot formation position error convergence diagram

Second, the simulation experiment of obstacle avoidance of multi-robot formation passing through the scattered obstacle area is conducted. In the experiment, some scattered obstacles are set on the paths through which the robot formations pass, and it is tested whether the robot formations can pass successfully. First step, the LiDAR carried by the robot formation's navigator detects the obstacle location and size data in front of it, and these data are judged by the program to be consistent with the scattered obstacle avoidance mode. Second step, the scattered obstacle avoidance mode is activated. Third step, complete the formation obstacle avoidance.

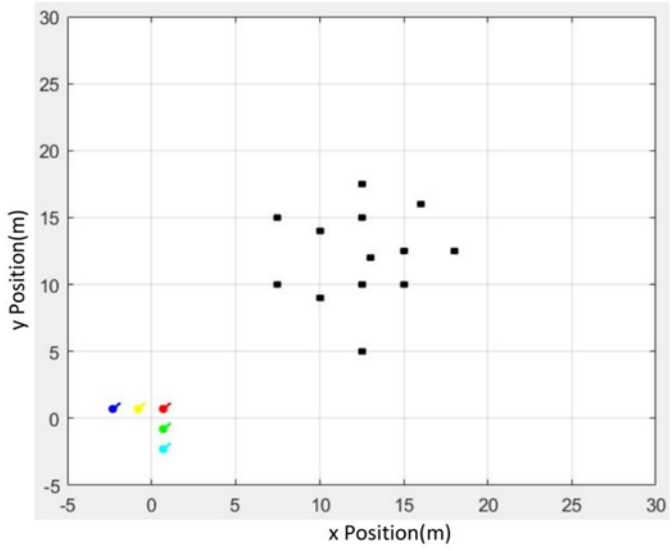

(a)

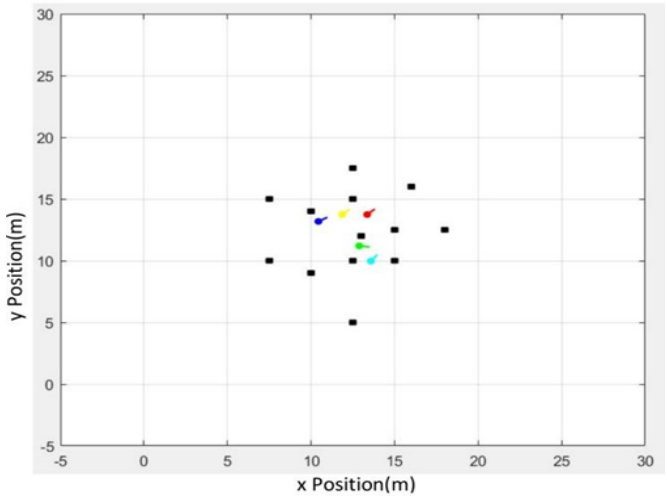

(b)

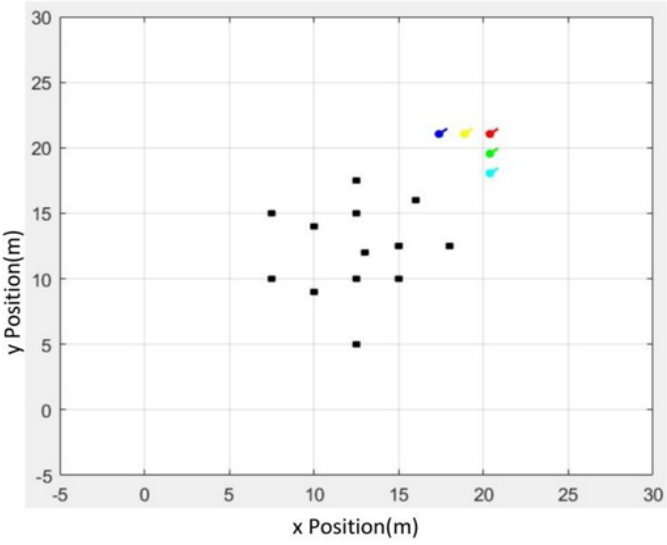

(c)

Figure13.Robot formation passing through scattered obstacles

(a). Initial Location Map. (b). Formation change process. (c). Formation completion chart

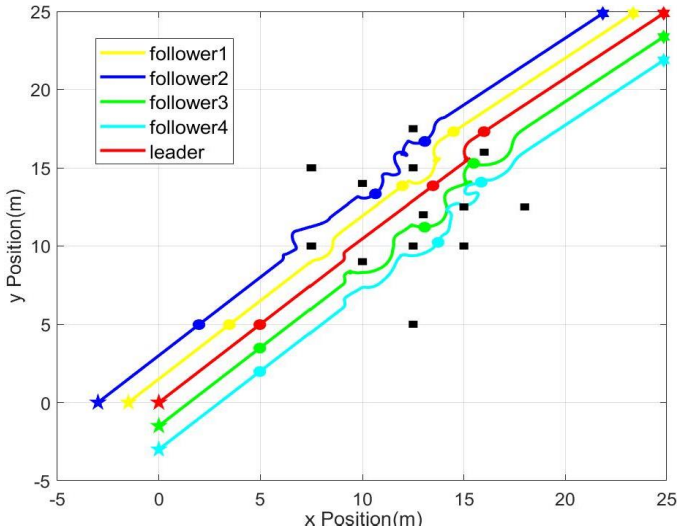

Figure14.Trajectory diagram of each robot

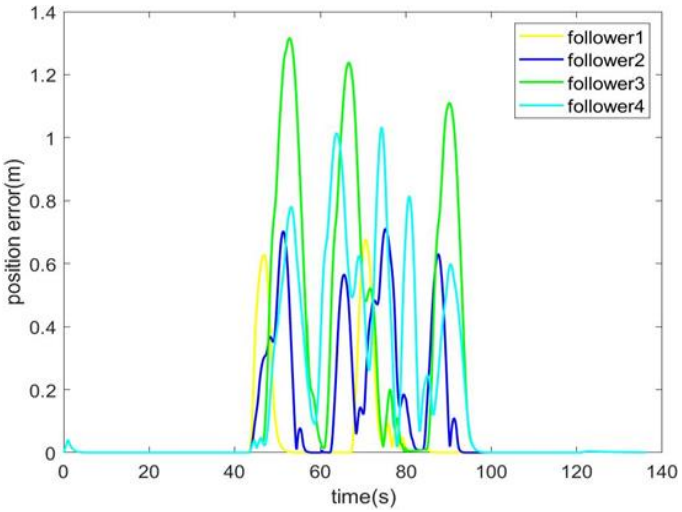

Figure15. Error diagram of each following robot position

Finally, in order to fully verify the performance of the strategy of dynamic formation transformation of mobile robot formations in complex scenarios proposed in this paper, simulation experiments are conducted. The initial formation shape of the robot formation is experimented with five robots forming a triangular initial formation as an example.

In this experiment, the initial formation of the robot formation is designed as a triangle, and in order to make the studied experimental scenario practical, the experimental environment is designed as shown in Figure 16, containing a total of four zones A, B, C, and D, E. The maximum passable width of each zone is different.

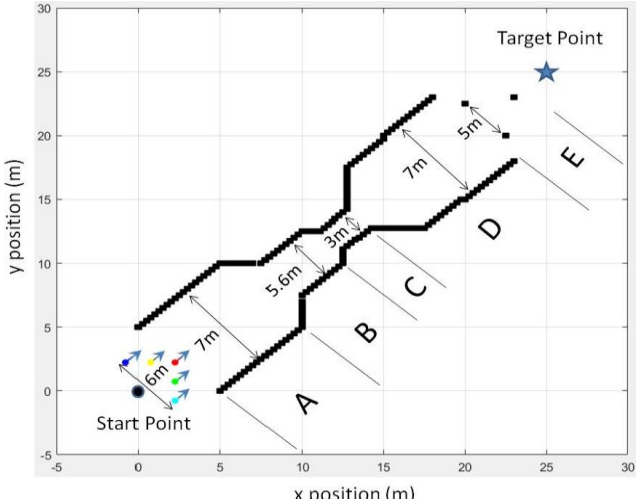

Figure16.Simulation experiment environment setup

In Figure 16, the obstacles are divided into continuous obstacle walls and scattered obstacles; the colored circles represent the robots, where the red cell is the leader robot and the rest are the following robots; the black dot represents the starting point and the star represents the target point; the arrow represents the direction of robot movement. The environment contains several common types of environments, such as narrow passage corridors, turning points and scattered obstacles and open spaces. The pilot robot detects the obstacles in the environment through its own laser sensors, and the robot formation dynamically optimizes the formation to pass the obstacle zone based on the detected obstacles and the strategy proposed in Section 5 of this paper. Figure 17-27 shows the dynamic formation optimization process when the robot formation passes through the experimental scenario.

A five-aircraft formation with an initial formation of a triangle is selected for simulation experiments. The formation starts at the starting point (x=0, y=0) to the target point of the formation (x=25, y=25). Ideal Formation Parameters: $H_{s1}^{d} = [1\ 0\ 0\ 0]$, $H_{s2}^{d} = [2\ 1\ 1.3\ \pi/4]$, $H_{s3}^{d} = [3\ 1\ 1.3\ -\pi/4]$, $H_{s4}^{d} = [4\ 1\ 2.6\ \pi/4]$, $H_{s5}^{d} = [5\ 1\ 2.6\ -\pi/4]$, Safe distance$ls$ = 0.3; Robot formation scaling factor ρ = 0.6.

Description of the formation crossing process.

In the interval $0 < x < 3$; $0 < y < 3$, it is the robot formation formation phase. In the 0-60s time interval, the mobile robot completes the initialization of the 5 robot formations according to the formation parameter matrix and the initial poses, forms a triangular formation shape, and keeps this formation in forward continuous motion.

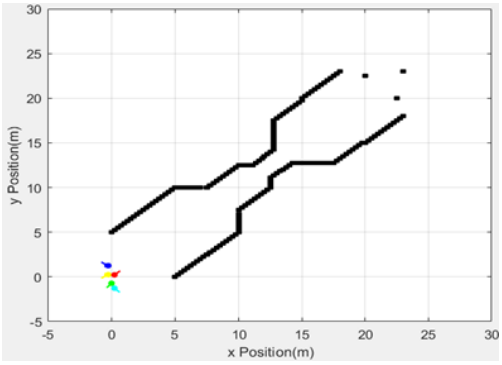

(a)

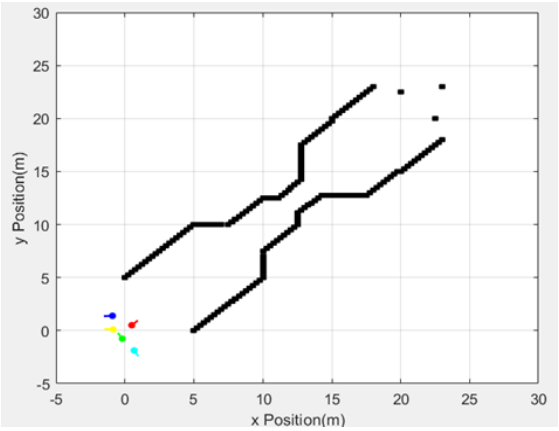

(b)

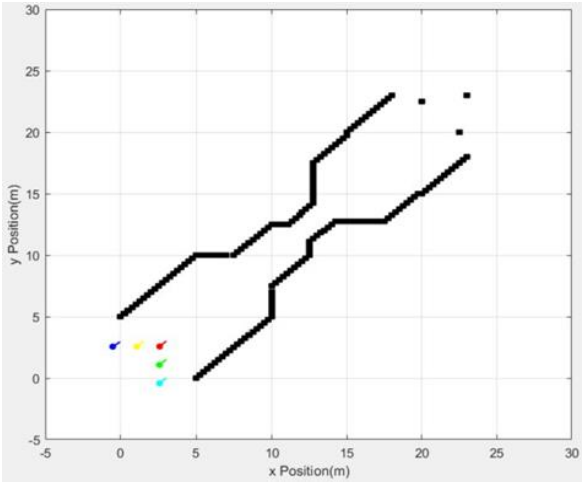

(c)

Figure17.Formation initialization

(a). Start formation. (b). Formation deformation. (c). Form a formation.

In the interval $3 < x < 10$; $3 < y < 10$, the mobile robot formation movement to the 100th s, the robot detects the appearance of obstacles. And judge its passable distance is D = 7m, and D＜D; so the formation according to the obstacle distance information with the formation operation, calculate to get the current formation stretching transformation parameter $\rho > 1$; the pilot robot leader set the formation transformation mode to $\sigma = 0$, and the formation adopts the formation keeping obstacle avoidance strategy to pass the obstacle area A with the current formation.

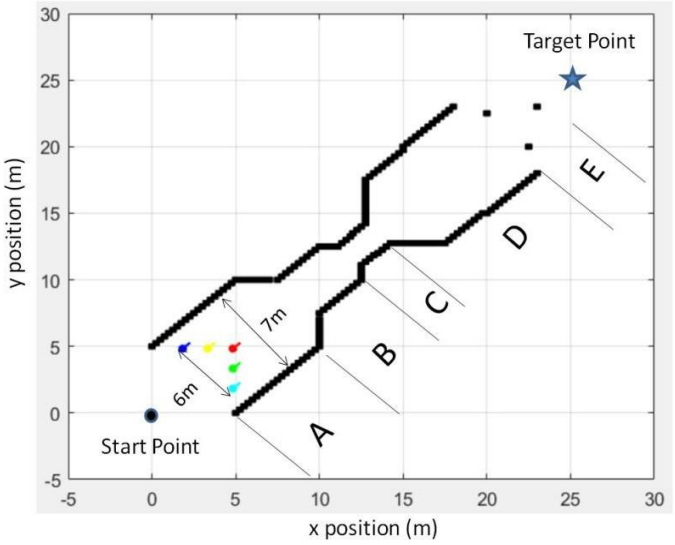

Figure18.Formation passes through the obstacle zone with no change

In the interval of $10 < x < 12.5$; $10 < y < 12.5$, the robot continues to move in the original formation after passing the obstacle area at this time. At x=10m, an obstacle area B is detected in front of it, at which time an obstacle avoidance strategy is adopted. Calculated its passable distance is D = 5.6m, and then according to the obstacle distance information and the current formation operation state, calculated the current formation expansion and contraction transformation parameter $\rho < \rho < 1$, at this time the pilot robot leader set the formation transformation mode for $\sigma = 1$, the formation using isomorphic deformation obstacle avoidance strategy, contraction formation length and formation angle. At this time, the distance between follower robot and the obstacle are greater than the robot avoidance safety distance*ls*, and each robot does not collide with each other, so that they pass the obstacle area B smoothly.

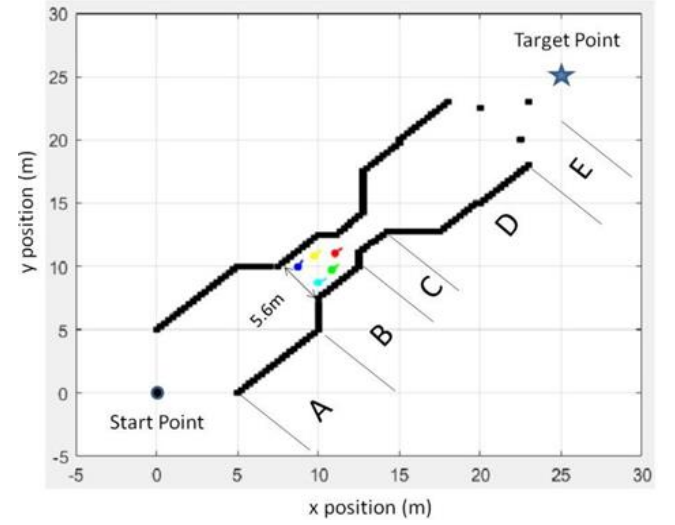

Figure19.Formation isomorphic deformation through obstacle zone

In the interval of $12.5 < x < 14$; $12.5 < y < 14$, at this time, the robot calculates the passable width D = 3m in the front obstacle area C. According to the obstacle information and the operation of the formation, the current formation expansion transformation parameter ρ < ρ is calculated, and the leader of the pilot robot sets the formation transformation mode to σ = 2, and the formation adopts the heterogeneous deformation obstacle avoidance strategy, at this time, the formation formation becomes linear transformation, so that the generation of its formation, and complete the formation of obstacle avoidance.

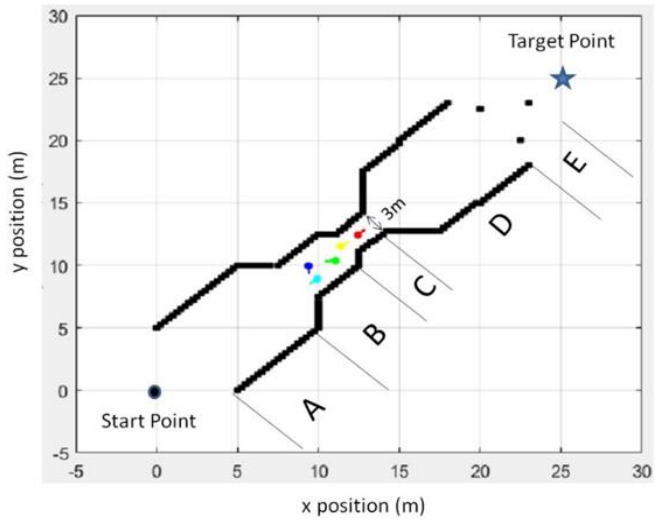

(a)

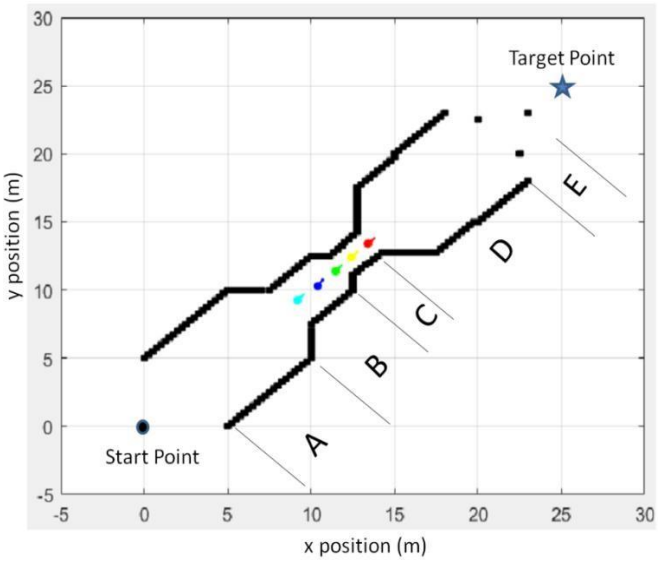

(b)

Figure20. Formation heterogeneous deformation through the obstacle zone

(a). Isomorphic deformation initiated. (b). Isomorphic deformation completed

In the interval of $14 < x < 17.5$; $14 < y < 17.5$, the robot detects that the obstacle appears, and its passable distance is D = 7m, and at this time the distance between follower robot and the obstacle are greater than the robot avoidance safety distance *ls*. Therefore, according to the obstacle distance information and the formation operation, the formation calculates and gets the current formation stretching transformation parameter $\rho > 1$, and the leader robot leader set the formation transformation mode to $\sigma = 0$, the formation to restore the original formation, formation to maintain the obstacle avoidance strategy, with the current formation through the obstacle area D.

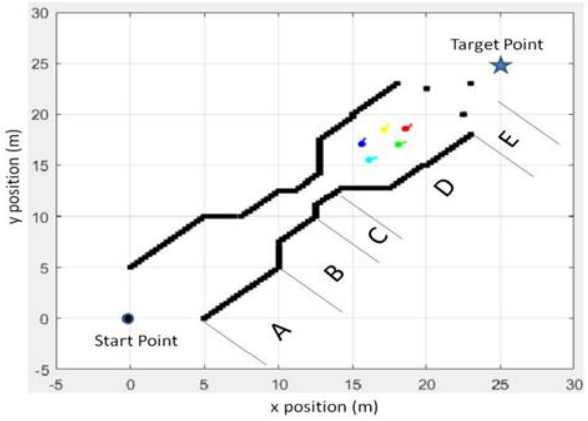

(a)

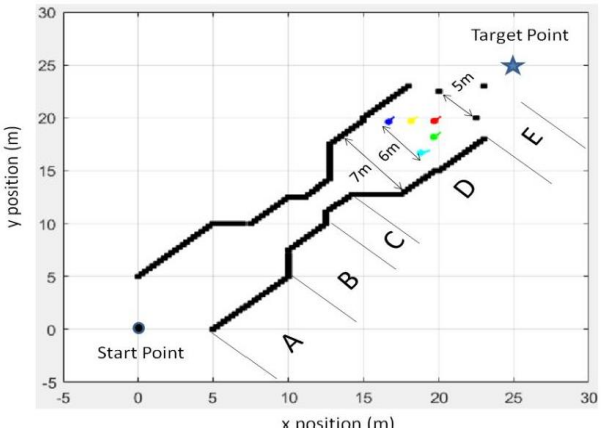

(b)

Figure21.Simulation diagram of robot formation heterogeneous formation recovery

(a). Transition from heterogeneous formation to homogeneous formation. (b). Return to original formation and maintain.

In the interval of $22.5 < x < 25$; $22.5 < y < 25$, the robot scans and gets multiple scattered obstacles in the obstacle area E ahead, the passable width D = 5m, and the size of the obstacles ＜ the width of the robot body, the formation operation mode is determined according to the obstacle information. First, calculate the current formation expansion transformation parameter $\rho < \rho$, the pilot robot leader set the formation transformation mode to $\sigma = 2$, second, the formation adopts the scattered obstacle avoidance strategy, at this time, the formation does not make a large change,

each robot avoid scattered obstacles to make its formation generation, and complete the formation to avoid obstacles.

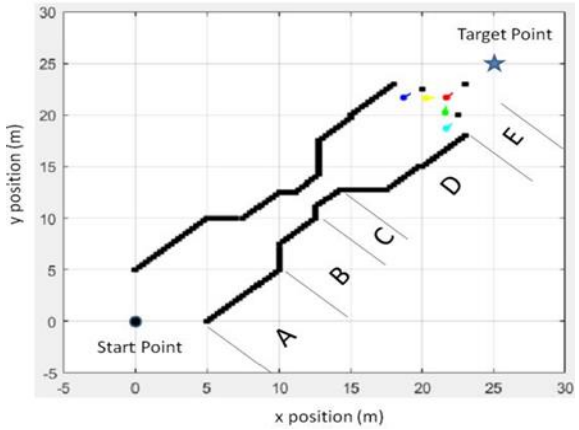

(a)

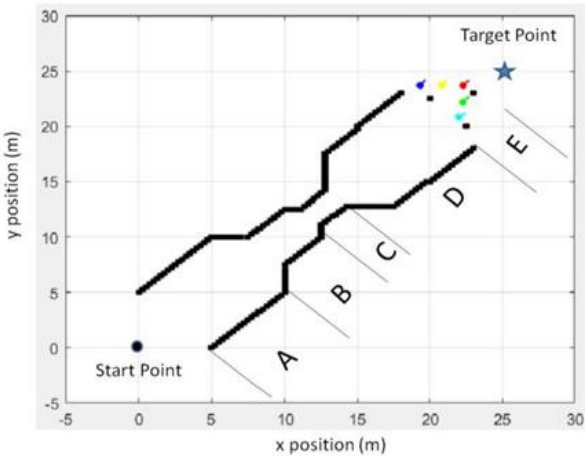

(b)

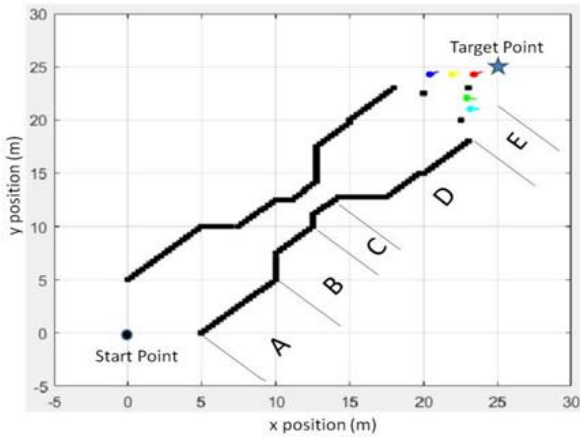

(c)

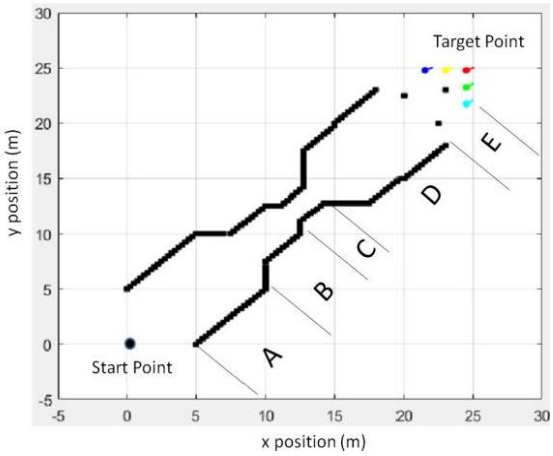

(d)

Figure22.Robot formation crossing a scattered obstacle.

(a). Scatter Crossing Start. (b). Crossing the first layer of obstacles. (c). Start the second layer of scattered obstacles over the barrier. (d). Formation through the obstacles to the finish line

In the interval of $22.5 < x \leq 25$m, the robot formation has passed the scattered obstacle zone, and in the absence of obs acles ahead, the formation starts to form the final target formation, and reaches the target point at t=600s to stop in a straight-line formation and complete the scheduled formation task.

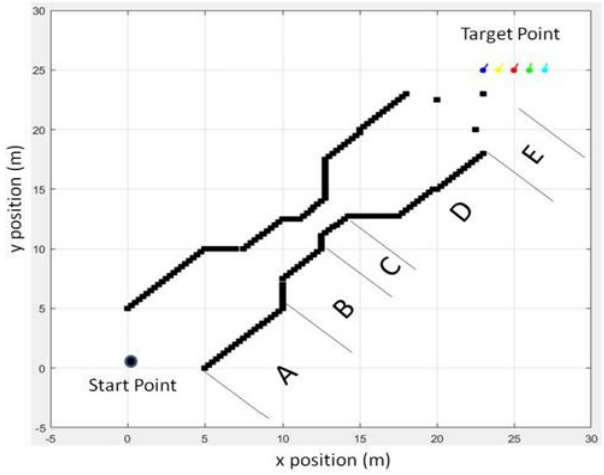

Figure23. Robot formation arrives at the target point to complete the process of crossing the barrier.

From the above experimental process, it can be seen that the robot formation can select the appropriate formation change mode independently according to the constraints of the environment and optimize the selection of a reasonable formation so that the robot formation can pass the experimental environment in Figure 16 smoothly, and finally pass the obstacle area and can return to the initial formation shape autonomously. In the above experimental process, the trajectory change curve of each robot is shown in Figure 24; the position error curve of follower1, follower2,

followerR3 and follower4 is shown in Figure 25.

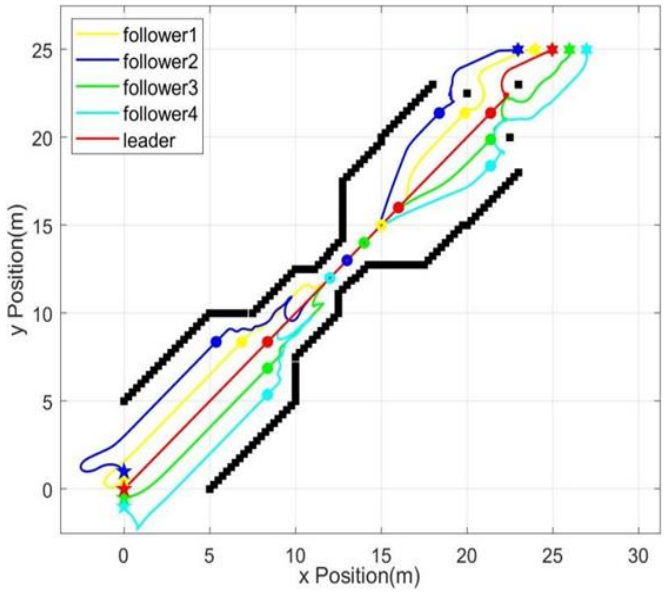

Figure24.Trajectory diagram of robot formation over obstacles

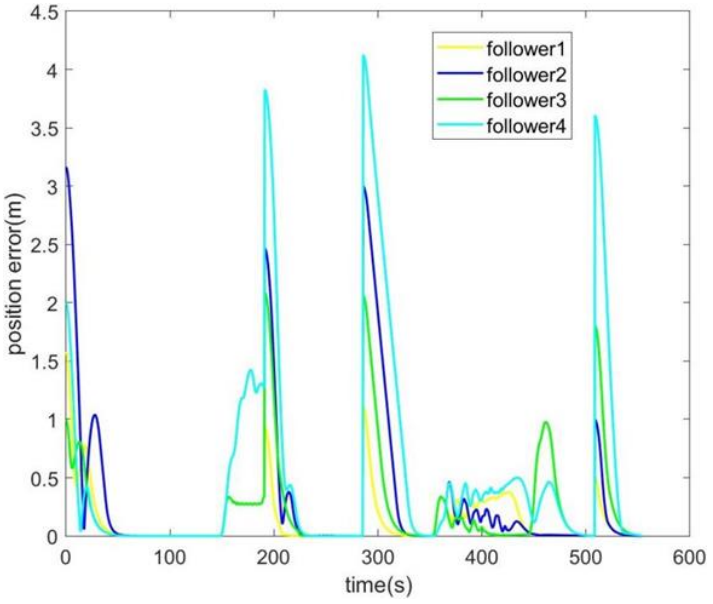

Figure25. Robot formation position error chart

From Figure 25, it can be seen that there is a large change information error at about 55s due to the change from the initialized linear formation to the triangular formation. Also at 150s, 300s and 400s, 500s, the robot formation changes formation due to environmental constraints, and at the moment of formation change, the position error in the X and Y directions suddenly increases to 3.8, 4.2 and 0.8 and 3.5, respectively, and the errors are the effect of changing formation when the robot formation encounters different obstacles. However, as the formation task continues,

all the position errors decrease rapidly when there are no obstacles, and the robot team re-form the optimized formation, and finally all the errors converge to 0. This indicates that the robot formation returns to the initial formation, which verifies the effectiveness of the dynamic formation optimization and obstacle avoidance strategy proposed in this paper.

5.2 Physical Experiments

This section builds a test environment for the multi-mobile robot formation experimental platform to carry out research related to multi-robot formation motion in a complex working environment and further test the practicality and effectiveness of the formation control algorithm and obstacle avoidance strategy proposed in this paper. The multi-mobile robot formation experimental platform uses a two-wheel differential speed mobile robot as the control individual and communicates with each robot using wireless LAN on the PC side. And based on the ROS development environment, two mobile robots are used as the main body of the formation, and the most representative heterogeneous formation transformation is adopted as the test target to complete the experimental verification of formation generation, maintenance, transformation and obstacle avoidance.

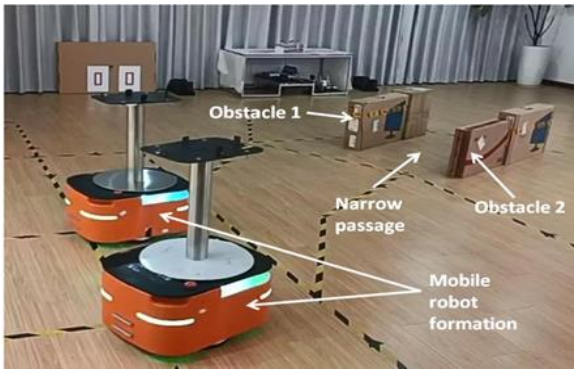

Figure26. A test environment of mobile robot formation

Physical experiments were designed to test the ability of robot formations to cross obstacles by deforming one of the most demanding narrow-aisle obstacle environments. Theoretically, if the robot formation can be adapted to this obstacle environment, the rest of the obstacle forms can also be adapted. Therefore, the test scenario basically covers the most demanding obstacle scenarios encountered by robot formations in actual factories, and is valid for illustration.

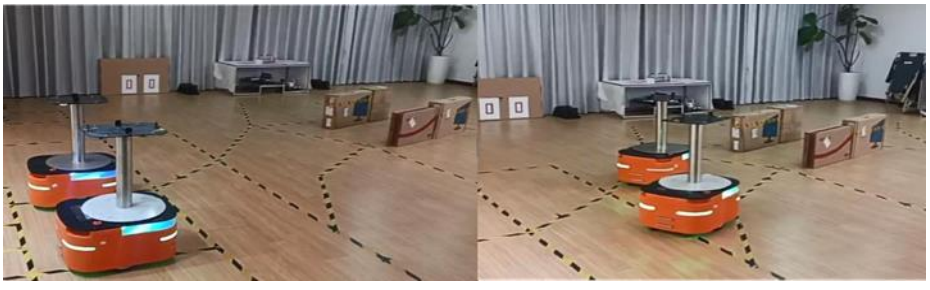

(a) *(b)*

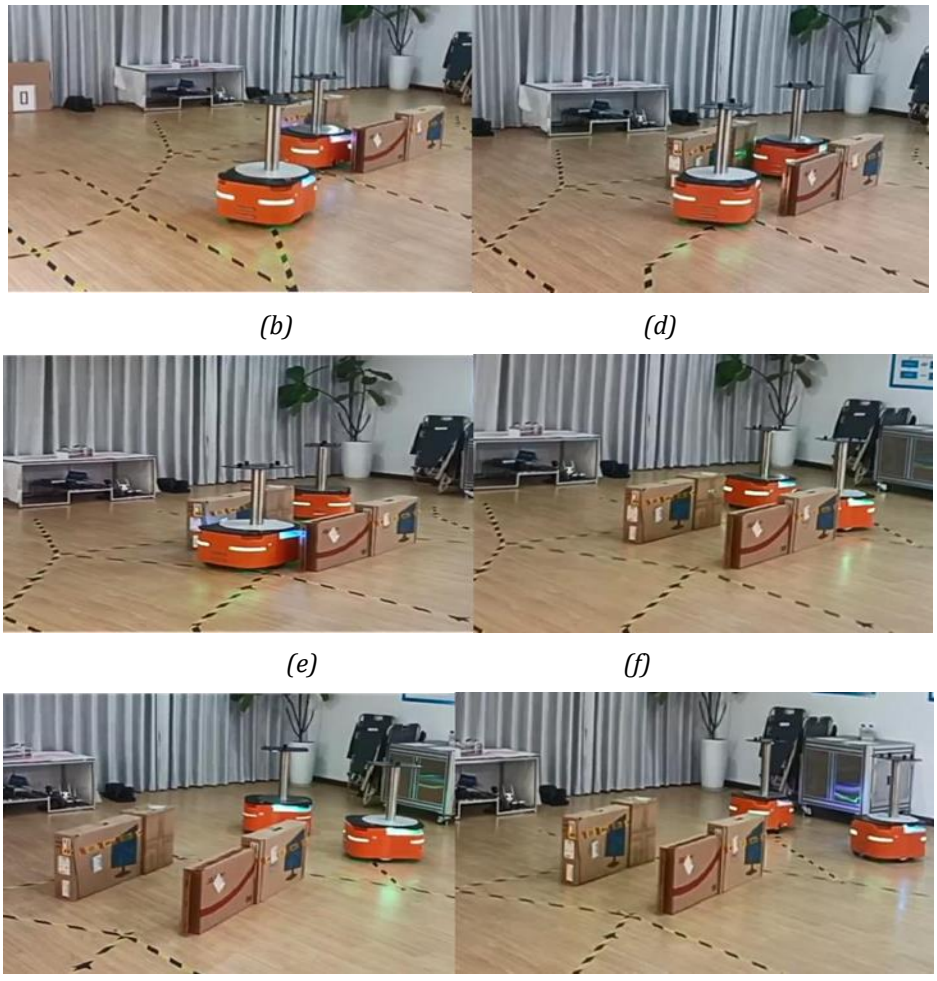

(b) *(d)*

(e) *(f)*

(g) *(h)*

Figure27.Experimental run diagram of mobile robot formation.

(a) Formation start point. (b). Formation heterogeneous deformation. (c). The Leader robot enters the narrow passage. (d). The Leader robot passes through the narrow passage. (e). Formation of Follower through the narrow passage. (f). Resume formation. (g). Robot formation stays in formation. (h). Robot formation reaches target point and stops.

The real-time operation of the formation is monitored at the PC. When t=0s, the robot on-board LiDAR starts to operate and each robot in the mobile robot formation is at the starting point position. As the formation advances, it continuously obtains data information about the surrounding obstacles. And in the operation to t=5s, the formation formed the initial formation, at this time, there is no obstacle in front of the mobile robot, the formation according to the obstacle distance information and the formation operation, calculate the current formation stretching transformation parameter $\rho > 1$; pilot robot leader set the formation transformation mode for $\sigma = 0$, the formation to maintain the formation to continue to move. When t=10s, the robot detects an obstacle in front of it and its passable distance is smaller than the width of

the formation, the controller calculates the current formation stretching parameter $\rho < \rho_t$, the leader sets the formation transformation mode to σ = 2, and the formation adopts the heterogeneous deformation obstacle avoidance strategy. The leader robot and the follower robot pass the narrow passage in turn. When t=20s, at this time, the robot formation passed the narrow channel obstacle area smoothly, and when the laser sensor monitored that no obstacle appeared in front, the formation executed the formation recovery command, and then moved forward in formation all the time. At t=25s, the pilot robot reaches the end position, issues the termination command, and the whole formation stops running.

In this section, the formation movement obstacle avoidance simulation experiments are conducted under the conditions of obstacle environment and different initial formation. The experimental results show that according to the formation transformation obstacle avoidance strategy proposed in this paper, the multi-mobile robot formation can select the most suitable formation to pass the obstacle area under different working environments. It proves that the multi-mobile robot formation control and transformation strategy proposed in this paper is effective.

6. Conclusions and Future Work

We design a strategy for mobile robot formation control and dynamic formation transformation in complex scenarios. Based on the introduction of the virtual robot's navigator-follower formation algorithm model and the formation quantization dataset, an efficient dynamic formation strategy for mobile robots with formation scaling factor ρ and formation dynamic transformation factor σ is finally developed. The strategy fully considers the environmental constraints in the formation avoidance process and the initial formation shape of the robot formation and dynamically selects four formation avoidance modes: scatter avoidance, formation maintenance, formation isomorphic transformation, and formation heterogeneous transformation, to dynamically obtain the optimal leader-follower topology that adapts to the complex obstacle environment. The simulation and physical experiment results show that the robot formation successfully completed formation holding, and formation change and successfully passed the set laboratory obstacles in the set obstacle environment. Therefore, this strategy can dynamically control the formation of robot groups performing formation tasks, and at the same time, it can adapt to the changes of the current environment to the maximum extent and has the ability to make robot formations switch to the optimal formation autonomously, which is a robot formation control method with practical value. However, one of the limitations of this method is that the distribution area of obstacles is too large, which is beyond the scanning range of the LiDAR carried by the robot. We will take two measures to deal with it, one is to replace the LiDAR with a wider scanning range, and the other is to adopt a step-by-step scanning method to obtain comprehensive obstacle data and then make a logical judgment on obstacle avoidance behavior. The future work will focus on two aspects: robot formation to avoid obstacles in a large area and to deal with the influence of dynamic obstacles.

Conflict of interest: The authors declare that they have no conflict of interest.

References

Akman, F. (2014). How to Utilize LJS Allen's" An Introduction to Mathematical Biology" in a Biomathematics Course. *Letters in Biomathematics*, *1*(2), 127-137. https://doi.org/10.30707/LiB1.2Akman

Arrichiello, F., Chiaverini, S., Indiveri, G., & Pedone, P. (2010). The null-space-based behavioral control for mobile robots with velocity actuator saturations. *The international journal of Robotics Research*, *29*(10), 1317-1337. https://doi.org/10.1177/0278364909358788

Chen, N., Wang, Y., & Jia, L. (2020). Multi-mobile robot leader-follower formation distributed control under switching topology. *2020 Chinese Control And Decision Conference (CCDC)*, 2673-2678. https://doi.org/10.1109/CCDC49329.2020.9164773

Chen, Y., Shi, X., & Li, B. (2022). Multi-Robot formation control based on improved virtual spring method. *2022 34th Chinese Control and Decision Conference (CCDC)*, 5614-5619. https://doi.org/10.1109/CCDC55256.2022.10033683

Deng, H., Xu, X., Ji, Y., Bai, Y., & Sun, X. (2022). D-Leader Control Algorithm for Multi-Robot Formation Transformation. *2022 5th International Conference on Artificial Intelligence and Big Data (ICAIBD)*, 488-494. https://doi.org/10.1109/ICAIBD55127.2022.9820142

Dudzik, S. (2020). Application of the motion capture system to estimate the accuracy of a wheeled mobile robot localization. *Energies*, *13*(23), 6437. https://doi.org/10.3390/en13236437

Fu, J., Tian, F., Chai, T., Jing, Y., Li, Z., & Su, C.-Y. (2018). Motion tracking control design for a class of nonholonomic mobile robot systems. *IEEE Transactions on Systems, Man, and Cybernetics: Systems*, *50*(6), 2150-2156. https://doi.org/10.1109/TSMC.2018.2804948

Gao, K., Xin, J., Cheng, H., Liu, D., & Li, J. (2018). Multi-mobile robot autonomous navigation system for intelligent logistics. *2018 Chinese Automation Congress (CAC)*, 2603-2609. https://doi.org/10.1109/CAC.2018.8623343

Hacene, N., & Mendil, B. (2021). Behavior-based autonomous navigation and formation control of mobile robots in unknown cluttered dynamic environments with dynamic target tracking. *International Journal of Automation and Computing*, *18*(5), 766-786. https://doi.org/10.1007/s11633-020-1264-x

Halima, M., Abdelouahab, H., & Yaakoub, T. M. (2018). Leader-follower formation control using PI controller. *2018 International conference on electrical sciences and technologies in Maghreb (CISTEM)*, 1-4. https://doi.org/10.1109/CISTEM.2018.8613569

Issa, B. A., & Rashid, A. T. (2019). A survey of multi-mobile robot formation control. *International Journal of Computer Applications*, *181*(48), 0975-8887. https://doi.org/10.5120/ijca2019918651

Jiamin, F., Jianwen, H., Ying, L., & Yufeng, X. (2022). Hierarchical control method for

multi-robot formation. *International Conference on Guidance, Navigation and Control*, 1637-1647. https://doi.org/10.1007/978-981-19-6613-2_160

Jiang, Q., & Yan, H. (2022). Leader-follower Motion Control of Two Line Following AGVs using PID Algorithm. *2022 IEEE 5th Advanced Information Management, Communicates, Electronic and Automation Control Conference (IMCEC)*, *5*, 445-449. https://doi.org/10.1109/IMCEC55388.2022.10020081

Lee, G., & Chwa, D. (2018). Decentralized behavior-based formation control of multiple robots considering obstacle avoidance. *Intelligent Service Robotics*, *11*(1), 127-138. https://doi.org/10.1007/s11370-017-0240-y

Li, G., & Chou, W. (2018). Path planning for mobile robot using self-adaptive learning particle swarm optimization. *Science China Information Sciences*, *61*(5), 052204. https://doi.org/10.1007/s11432-016-9115-2

Li, G., St-Onge, D., Pinciroli, C., Gasparri, A., Garone, E., & Beltrame, G. (2019). Decentralized progressive shape formation with robot swarms. *Autonomous Robots*, *43*(6), 1505-1521. https://doi.org/10.1007/s10514-018-9807-5

Li, S. W. (2021). Design and Implementation of Improved Leader Follower Formation Control and Tracking Algorithm Based on Global Reference Framework in Network Environment. *2021 4th International Conference on Intelligent Robotics and Control Engineering (IRCE)*, 20-23. https://doi.org/10.1109/IRCE53649.2021.9570881

Liang, Q., Sun, T., & Wang, D. (2017). Time-varying reliability indexes for multi-AUV cooperative system. *Journal of Systems Engineering and Electronics*, *28*(2), 401-406. https://doi.org/10.21629/JSEE.2017.02.20

Liang, X., Wang, H., Liu, Y.-H., Liu, Z., & Chen, W. (2020). Leader-following formation control of nonholonomic mobile robots with velocity observers. *IEEE/ASME Transactions on Mechatronics*, *25*(4), 1747-1755. https://doi.org/10.1109/TMECH.2020.299099110.1109/TMECH.2020.2990991

Liu, G.-P., & Zhang, S. (2018). A survey on formation control of small satellites. *Proceedings of the IEEE*, *106*(3), 440-457. https://doi.org/10.1109/JPROC.2018.2794879

Liu, T., & Jiang, Z.-P. (2013). Distributed formation control of nonholonomic mobile robots without global position measurements. *Automatica*, *49*(2), 592-600. https://doi.org/10.1016/j.automatica.2012.11.031

Park, B. S., & Yoo, S. J. (2021). Connectivity-maintaining and collision-avoiding performance function approach for robust leader–follower formation control of multiple uncertain underactuated surface vessels. *Automatica*, *127*, 109501. https://doi.org/10.1016/j.automatica.2021.109501

Rabelo, M. F. S., Brandão, A. S., & Sarcinelli-Filho, M. (2018). Centralized control for an heterogeneous line formation using virtual structure approach. *2018 Latin American Robotic Symposium, 2018 Brazilian Symposium on Robotics (SBR) and 2018 Workshop*

on Robotics in Education (WRE), 135-140. https://doi.org/10.1109/LARS/SBR/WRE.2018.00033

Raghuwaiya, K., Sharma, B., & Vanualailai, J. (2018). Leader-follower based locally rigid formation control. *Journal of Advanced Transportation*, *2018*, 1-14. https://doi.org/10.1155/2018/5278565

Roy, D., Chowdhury, A., Maitra, M., & Bhattacharya, S. (2018). Multi-robot virtual structure switching and formation changing strategy in an unknown occluded environment. *2018 IEEE/RSJ International Conference on Intelligent Robots and Systems (IROS)*, 4854-4861. https://doi.org/10.1109/IROS.2018.8594438

Saleh, A. L., Hussain, M. A., & Klim, S. M. (2018). Optimal trajectory tracking control for a wheeled mobile robot using fractional order PID controller. *Journal of University of Babylon for Engineering Sciences*, *26*(4), 292-306. https://doi.org/10.29196/jubes.v26i4.1087

Tran, V. P., Garratt, M., & Petersen, I. R. (2020). Switching time-invariant formation control of a collaborative multi-agent system using negative imaginary systems theory. *Control Engineering Practice*, *95*, 104245. https://doi.org/10.1016/j.conengprac.2019.104245

Wasik, A., Pereira, J. N., Ventura, R., Lima, P. U., & Martinoli, A. (2016). Graph-based distributed control for adaptive multi-robot patrolling through local formation transformation. *2016 IEEE/RSJ International Conference on Intelligent Robots and Systems (IROS)*, 1721-1728. https://doi.org/10.1109/IROS.2016.7759276

Yaghmaei, M., & Abedi, M. (2018). Backstepping Sliding-Mode Formation Control of Electrically Driven Nonholonomic Mobile Robots. *Electrical Engineering (ICEE), Iranian Conference on*, 811-815. https://doi.org/10.1109/ICEE.2018.8472525

Yan, C., & Fang, H. (2019). A new encounter between leader–follower tracking and observer-based control: Towards enhancing robustness against disturbances. *Systems & Control Letters*, *129*, 1-9. https://doi.org/10.1016/j.sysconle.2019.04.010.2019.04.010

Yan, X., Jiang, D., Miao, R., & Li, Y. (2021). Formation control and obstacle avoidance algorithm of a multi-USV system based on virtual structure and artificial potential field. *Journal of Marine Science and Engineering*, *9*(2), 161. https://doi.org/10.3390/jmse9020161

Yin, H., Guo, S., & Liu, M. (2022). A virtual linkage-based dual event-triggered formation control strategy for multiple amphibious spherical robots in constrained space with limited communication. *IEEE Sensors Journal*, *22*(13), 13395-13406. https://doi.org/10.1109/JSEN.2022.3175715